This is a preprint, the final version is subject to change, of the American Mineralogist (MSA)
Cite as Authors (Year) Title. American Mineralogist, in press.
(DOI will not work until issue is live.) DOI: http://dx.doi.org/10.2138/am-2016-5449

# Revision 1: High Pressure Behavior of the Polymorphs of FeOOH

Mary M. Reagan[1], Arianna E. Gleason[2], Luke Daemen[3], Yuming Xiao[4], Wendy L. Mao[1,5]

[1]Department of Geological Sciences, Stanford University, Stanford, CA 94305 [2]Shock and Detonation Physics, LANL, Los Alamos, NM 87545 [3] Spallation Neutron Source, Oak Ridge National Laboratory, Oak Ridge, TN, 37830 [4]Advanced Photon Source, Argonne National Laboratory, Lemont, IL, 60439 [5]Photon Science, SLAC National Accelerator Laboratory, Menlo Park, CA 94025

**Abstract:**

The high-pressure structural and electronic behavior of α-, β-, and γ-FeOOH were studied in-situ using a combination of synchrotron X-ray diffraction (XRD) and X-ray emission spectroscopy (XES). We monitored α-FeOOH by XES as a function of pressure up to 85 GPa and observed an electronic spin transition that began at approximately 50 GPa, which is consistent with previous results. In the γ-FeOOH sample, we see the initiation of a spin transition at 35 GPa that remains incomplete up to 65 GPa. β-FeOOH does not show any indication of a spin transition up to 65 GPa. Analysis of the high-pressure XRD data shows that neither β-FeOOH nor γ-FeOOH transform to new crystal structures, and both amorphize above 20 GPa. Comparing our EOS results for the β and γ phases with recently published data on the α and ε phases, we found that β–FeOOH exhibits distinct behavior from the other three polymorphs, as it is significantly less compressible and does not undergo a spin transition. A systematic examination of these iron hydroxide polymorphs as a function of pressure can provide insight into the relationship between electronic spin transitions and structural transitions in these OH- and $Fe^{3+}$ bearing phases



Always consult and cite the final, published document. See http:/www.minsocam.org or GeoscienceWorld

that may have implications on our understanding of the water content and oxidation state of the mantle.

## Introduction:

Iron hydroxides, including FeOOH and its polymorphs, are common on the surface of the Earth, where they are abundant in soils, aquifers and sediments. FeOOH has four polymorphs, three of which are naturally occurring: goethite (α-FeOOH), akaganeite (β-FeOOH), and lepidocrocite (γ-FeOOH), A fourth polymorph, ε–FeOOH, can be synthesized at high pressure (Bolotina et al., 2008, Gleason et al., 2008, Voigt et al., 1981). Goethite is the thermodynamically stable phase at ambient conditions, whereas akaganeite is rare and forms in Cl-rich environments like hot brines and rust in marine environments. Lepidocrocite occurs in rocks, soils and rust and is often an oxidation product of $Fe^{2+}$. Their structures consist of corner-linked double bands of $FeO_3(OH)_3$ octahedra (Figure 1). α-FeOOH has double bands of edge sharing octahedra that form 2x1 channels. β-FeOOH also has double bands; however, they are arranged in a circular shape forming large 2x2 channels, which are stabilized by the presence of a variable molecule or ions such as $H_2O$, $OH^-$, $Cl^-$, or $NO_3^-$. The γ-FeOOH bands are connected via hydrogen bonds (OH-O) and form corrugated 2d layers perpendicular to the b-axis. The high-pressure ε-FeOOH phase is a slightly distorted rutile structure with corner-linked single bands of edge-shared octahedra parallel to the c-axis (Otte et al., 2009). It is isostructural with δ-AlOOH, a phase that may transport hydrogen deep within the planet and potentially down to the core-mantle boundary (Sano et al., 2004; Suzuki, 2010).

Based on crystal field theory, the distribution of electrons in the *d* orbitals in transition



Always consult and cite the final, published document. See http:/www.minsocam.org or GeoscienceWorld

metal complexes depends on the ligand field geometry and the metal *d*-electron configurations. The spin state of iron is determined by the difference between the energy levels of $\Delta_c$ (the crystal field splitting parameter) and the spin pairing energy ($\Lambda$). Under ambient conditions, $\Delta_c$ for most octahedrally coordinated iron compounds is lower than $\Lambda$. This results in favorable energetic conditions where 3*d* electrons occupy both the $t_{2g}$ orbitals and the higher energy $e_g$ orbitals with unpaired spins. With increasing pressure, the crystal field splitting energy increases with respect to the spin pairing energy, this can result in the spin pairing of the electrons in the lower energy $t_{2g}$ orbital. Thus spin transitions in iron in lower mantle minerals may result in significant changes in their physical and chemical properties (Speziale et al., 2005)-- including their density, bulk modulus, seismic velocities, electrical conductivity, radiative heat transfer, and element partitioning (Lin et al., 2013; Lin et al., 2008; Lin et al., 2007; Speziale et al., 2005; Stackhouse et al., 2007). Previous work (Gleason et al., 2013; Xu et al., 2013) showed that spin transitions take place in α-FeOOH and ε-FeOOH. Gaining insight into the high pressure behavior and spin state of the polymorphs of FeOOH can improve our understanding of more complex hydrogen bearing compounds that may be common in the Earth's deep interior (Williams et al., 2001).

## Experimental methods:

### Sample synthesis:

α, β and γ- FeOOH were synthesized using the methods in Schertmann (2000), with β-FeOOH was prepared following a slight modification. After dissolving 54.6 g FeCl3.6H2O (0.2 mol) in 200 mL of deionized water in a 500 mL polyethylene bottle, a solution of 6 g NaOH in 120 mL deionized water was added to the iron chloride solution.



Always consult and cite the final, published document. See http:/www.minsocam.org or GeoscienceWorld

A brown precipitate forms, which redissolves upon shaking. The resulting clear, brown solution is allowed to age at room temperature for 3 days, at which point 40 mL of a 10 M solution of NaOH in deionized water is added rapidly with vigorous stirring. The resulting solution is heated to 80 °C in the closed polyethylene bottle until a brown precipitate starts appearing. This requires 6 to 7 days. After the solution becomes a cloudy suspension, heating is continued for 4 days. The suspension of β-FeOOH is difficult to filter by conventional means and the solid is separated from the supernatant liquid by centrifugation. The solid is washed repeatedly by resuspension in 250 mL of water, stirring for several minutes, and centrifugation. This washing operation is repeated several times until the supernatant liquid no longer gives a positive test for chloride by precipitation with a silver nitrate solution. The solid material is then dried in a vacuum oven at 40 °C.

**Chloride analysis:**

The simplest method for chloride determination is Mohr's titration with aqueous silver nitrate, using sodium chromate as an indicator (Skoog et al.,1996). The method requires to bring β-FeOOH in solution. Hydrochloric acid dissolves β-FeOOH quite readily, but, obviously, cannot be used for the sample preparation in the determination of chloride in β-FeOOH. Furthermore, any Broensted acid used to dissolve β-FeOOH cannot introduce an anion that forms an insoluble salt with silver. Nitric acid would be ideal, but does not dissolve β-FeOOH at or above room temperature. Sample preparation proceeded as follows. A small amount of β-FeOOH (circa 50 mg) was placed in the teflon liner of a 23 mL Parr autoclave. Deionized water (8mL) was placed in the vessel, then 4 mL of concentrated nitric acid. Four drops of triflic acid were added, after which the autoclave



Always consult and cite the final, published document. See http:/www.minsocam.org or GeoscienceWorld

was sealed and placed in an oven. The temperature was raised progressively to 180 °C over a period of one day and the autoclave was kept at this temperature for two more days. The autoclave was allowed to cool down to room temperature before opening. The teflon liner contained a clear liquid with no visible traces of solid. This method of sample preparation has the advantage of preventing any loss of chlorine in the form of HCl. The clear solution was transferred to a 250 mL beaker, diluted with 100 mL of water, and pH was raised to about 6 with the addition of small amounts of sodium bicarbonate. At this pH, iron precipitates as iron hydroxide. This solid is filtered, washed carefully, and the filtrate is then used for Mohr titration with a 20 mM aqueous solution of silver nitrate. Three samples were prepared in this fashion for chloride determination. If a nominal formula for β-FeOOH is assumed to be, Fe O (OH)_x Cl_(1-x), then the titration results gave x = 0.84 +/- 0.015, which indicates that some 15% of the hydroxide ions are replaced by chloride ions in the β-FeOOH structure. This is consistent with previous observations.

**Sample Preparation**

Powdered samples of synthesized α-FeOOH, β-FeOOH, and γ-FeOOH (Gerth, 1990; Kosmulski et al., 2003; Wang et al., 2004) were loaded separately into a beryllium (for XES) or tungsten and stainless steel (for XRD) gasket. For α-FeOOH, a 100 μm hole served as the sample chamber while a sample chamber of 120 μm was used for β-FeOOH, and γ-FeOOH. All samples were compressed between 300 μm diamond culets in a symmetric diamond anvil cell (DAC). No pressure-transmitting medium was used for the XES experiments to maximize signal, and silicone oil was used for the XRD experiments. Ruby and gold (Mao et al., 1978, Heinz et al., 1984) were used as pressure



Always consult and cite the final, published document. See http:/www.minsocam.org or GeoscienceWorld

115 calibrants for the XRD experiments, while ruby only was used for the XES experiments.

116 **Synchrotron X-ray Experiments**

117 Angle-dispersive powder XRD measurements were collected at beamline 12.2.2 of the
118 Advanced Light Source (ALS), Lawrence Berkeley National Laboratory (LBNL) where a
119 wavelength of 0.4959 Å x-rays with a beam spot of 10 x 10 μm were used and a smaple
120 to detector distance of 354.41 mm, and at HP-CAT, beamline 16-BM-D at the Advanced
121 Photon Source (APS), Argonne National Laboratory (ANL) where a wavelength of
122 0.4246 Å x-rays with a beam spot size of 5 x 5 μm were used and a sample to detector
123 distance of 320.66mm. XRD data for β-FeOOH was collected at APS, while data for γ-
124 FeOOH was collected at ALS. All data were collected on a MAR345 image plate and cell
125 parameter refinements were carried out using the MAUD program (Lutterotti et al.,
126 1997). The Fe Kβ XES spectra of α, β, and γ-FeOOH were collected at HP-CAT,
127 beamline 16ID-D, APS, ANL. The incident X-ray energy were monochromatized using a
128 Si(111) double crystal monochromator and was centered at 11.3 keV, and the scans were
129 set relative to 7.058 keV with a range of -40 to +25 eV. Table 2 provides a summary of
130 the experimental techniques.

131 **Results:**

132 **X-ray Diffraction:**

133 The 2D patterns were integrated using Fit 2D (Hammersley, 1998) and Le Bail
134 refinements of the integrated patterns were carried out to determined the unit cell
135 volumes at each pressure using MAUD program (Lutterotti et al., 1997). Background fits
136 were determined using a 3$^{rd}$ order polynomial that was manually set. Lattice parameters



Always consult and cite the final, published document. See http:/www.minsocam.org or GeoscienceWorld

were refined to a goodness of fit of 0.6 % (β) and 0.5 % (γ) as determined by MAUD. For γ-FeOOH, the (200) peak was used to constrain the *a* lattice parameter at each pressure step. Analysis of the XRD data shows that neither β-FeOOH or γ-FeOOH undergo any first order structural transitions over the pressure range studied, and both show evidence of amorphization above ~20 GPa (Figures 2, 3). We fit our pressure-volume data to a 2$^{nd}$ order Birch-Murnaghan equation of state (EOS) (Birch, 1978), and found that β-FeOOH has a $V_0$ of 336.6(3) Å$^3$, and $K_0$ value of 284(1) GPa. The γ-FeOOH phase has a $V_0$ of 147.76(2) Å$^3$ and a $K_0$ value is 104(1) GPa. These results are summarized in Table 1 and plotted in Figures 4 and 5, where the β and γ phases are compared with recently published work on the α- (Xu et al., 2013) and ε- (Gleason et al., 2013) phases.

**X-ray Emission Spectroscopy:**

The spin state of iron is monitored through Kβ XES, where a *K* shell electron core-hole is created when an electron absorbs an X-ray photon and is emitted from the atom. This is followed by a 3*p* electron falling to the *K* shell, and in transition metals (e.g., iron), an exchange interaction occurs between the 3*p* core hole and the unpaired 3*d* shell when a material is in high spin. The resultant emission spectrum consists of $K\beta_{1,3}$ peak and the smaller satellite peak, Kβ' that arises from the exchange interaction between 3*p* core hole and the 3*d* shell. We monitored α-FeOOH as a function of pressure up to 85 GPa and observed that it undergoes a spin transition beginning at ~50 GPa. This is seen in the evolution of the Kβ emission spectra where a clear reduction of Kβ' was observed (Figure 6). Each spectrum at a given pressure was summed and normalized using the integrated absolute difference method (IAD) (Mattila et al., 2007). Our IAD values indicate the high to low spin transition occurred over a range of 50-70 GPa (Figure 7).



Always consult and cite the final, published document. See http:/www.minsocam.org or GeoscienceWorld

This is in good agreement with a previous study that found a high to low spin cross over above 45 GPa (Xu et al., 2013). In the γ-FeOOH sample, we see a spin transition beginning at 35 GPa that remains incomplete to 65 GPa, which is evidenced by the partial reduction of the satellite peak (Figure 8). The β-FeOOH sample does not show any indication of a spin transition for pressures up to the highest pressure investigated, 65 GPa (Figure 9). We note that although both the β and the γ phases become amorphous at pressures above 20 GPa, the study of the spin state provides valuable information about the electronic configuration despite the loss of the long-range order.

**Discussion**:

At ambient pressure, the polymorphs of FeOOH are made up of asymmetric octahedra of $Fe^{3+}_{HS}$ $(O_1\text{-}H)_3(O_2\cdots H)_3$, with two distinct types of oxygen bonding, the shorter $O_1$-H and the longer $O_2\cdots H$. These bond lengths vary as they are subjected to pressure, with the length of the Fe-$O_1$ and Fe-$O_2$ bonds and the $O_1 \cdots O_2$ distance affecting the spin state. These previous studies (Xu et al., 2013) have also linked the electronic spin transition with the symmetrization of the hydrogen bonds in α-FeOOH. Increasing pressure leads to a shift in the proton position where the $O_1$-H and $O_2\cdots H$ bonds become more equal in length. Single-crystal studies show that at 45 GPa, there is a large drop in volume that corresponds to a reduction of the $Fe^{3+}$ radius (Xu et al., 2013). The asymmetry of the polyhedra is reduced as the Fe-$O_1$ and Fe-$O_2$ bonds are close to equal and the $O_1$-Fe-$O_2$ angle becomes 180°. α-FeOOH undergoes a spin transition at 47 GPa, with hydrogen bond symmetrization occurring at pressures above 50 GPa. In this case, the spin crossover leads to the hydrogen bond symmetrization (Xu et al., 2013). ε- FeOOH's



Always consult and cite the final, published document. See http:/www.minsocam.org or GeoscienceWorld

182 behavior shows an opposite order of events, with increasing pressure: the spin transition
183 starts at 49 GPa, while DFT calculations show that its hydrogen bonds symmetrize at a
184 lower pressure of 43 GPa. The hydrogen bond symmetrization results in the elongation of
185 the $O_1$-H and the compression of $O_2$···H, with hydrogen reaching an equidistant position
186 at ~1.2 Å and the $O_1$-H···$O_2$ bond angle adjusting to 180°. (Gleason et al., 2013).
187 Interestingly, previous DFT calculations show that in γ- FeOOH the $O_1$-H remain
188 constant at ~ 1.2 Å, while at 15 GPa, the $O_2$···H bond reduces from 3.1 Å to 2.9 Å. (Otte
189 et al., 2009). Its spin transition begins at higher pressure of 36 GPa where the sample is
190 amorphous and remains incomplete up to 65 GPa, the highest pressure we studied (Figure
191 8). Previous DFT calculations for β–FeOOH, indicate that its O-H bonds remain nearly
192 constant with increasing pressure up to 20 GPa (Otte et al., 2009). The DFT calculations
193 for the β and γ phases only go up to 20 GPa, so it is not known how their bond lengths
194 are changing at higher pressures, or at the onset of the spin transition in γ-FeOOH.

195 The β phase has a distinct behavior when compared to the other polymorphs of FeOOH.
196 It is the only polymorph that does not undergo an electronic spin transition over the range
197 of pressures studied. DFT calculations for β–FeOOH show that its oxygen-hydrogen
198 bonds remain constant with increasing pressure. It is significantly less compressible as
199 indicated by its higher $K_0$ value compared to the other polymorphs (Table 1). Its
200 electronic configuration remaining in high spin maybe related to its incompressibility
201 thus leading to polyhedra remaining more asymmetric and less compressed. There is
202 small amount of $Cl^-$ present in the β–FeOOH that stabilizes the 2x2 channels in its
203 structure and is therefore less compressible allowing it to remain in the high spin state



Always consult and cite the final, published document. See http:/www.minsocam.org or GeoscienceWorld

with increasing pressure. β–FeOOH and to a lesser extent γ-FeOOH also have a larger volume per formula unit when compared with α– and ε-FeOOH (Table 1, Figure 4). This may also contribute to why both β- and γ-FeOOH become amorphous at high pressure as they are energetically less stable than their denser polymorphs but the transition is hindered until they become mechanically unstable and amorphize. Future computational work to look at the hydrogen bonding as a function of pressure for β- and γ–FeOOH would provide further insight into the high-pressure behavior of these polymorphs.

## Implications:

It has been proposed that the electronic transition in $Fe^{3+}$ and the symmetrization of the hydrogen bond are closely connected for the FeOOH polymorphs (Gleason et al., 2013; Xu et al., 2013). The spin transition is driven by the decreasing Fe-$O_{1, 2}$ bonds and the change in the $O_1 \cdots O_2$ distance, which leads to an environment that increases the crystal field splitting parameter until it is more energetically favorable for the low spin state. In full spin transitions, this change is often accompanied by the hydrogen bond symmetrization. In both α–FeOOH and ε-FeOOH, a complete spin transition is coupled with hydrogen bond symmetrization. In γ-FeOOH, there is only a partial shift in its hydrogen atom, which maybe a reflection that the polymorph does not undergo a full spin transition. β–FeOOH also shows this connection with its bond length remaining relatively unchanged and a lack of a spin transition. Hydrogen bond symmetrization has also been observed at high pressure in α–AlOOH, which is isostructural with α–FeOOH and is present in subducting sedimentary rocks. Its hydrogen bonds become increasingly more symmetric up through the studied range of 50 GPa (Friedrich et al., 2007). Other oxy-



Always consult and cite the final, published document. See http:/www.minsocam.org or GeoscienceWorld

hydroxide transition metal compounds may also undergo hydrogen bond symmetrization when subjected to high pressure, and further work is needed to understand the possible connection between hydrogen bond symmetrization and electronic structure changes. The symmetrization of hydrogen bonds is expected to have an effect on the elasticity and plasticity of hydrogen-bearing materials. Quantifying the stability of the hydrogen bonds in relation to hydrous Fe-bearing minerals with the potential for undergoing an electronic transition can give insight into the behavior of hydrogen in an Fe-rich environment at deep Earth conditions (Benoit et al., 1998; Gilli et al., 2009; Friedrich et al., 2007; Holzapfel, 1972; Xu et al., 2013).

Iron is the most abundant transition metal in the deep Earth, and iron-bearing materials may transition to a low spin state at shallower depths as their water content increases (Frost & McCammon, 2008; Otte et al., 2009; Xu et al., 2013). The experimental work on the polymorphs of FeOOH indicate that increasing pressure can have dramatic effects on the electronic state and the crystal structure, including the nature of the hydrogen bonds. This effect may be ubiquitous in transition metal bearing compounds that contain water- and relevant to the deep Earth. Ferric iron bearing silicates may play an important role in transporting water into the deep mantle. Changes to their spin states and hydrogen bonds might then have an influence on the water dynamics and balance within the deep Earth (Williams and Hemley, 2001). This has implications for the oxidation state of the Earth's mantle, where the redox state controls $Fe^{3+}$ and $OH^-$ content within minerals, as well as, water partitioning in fluids/melts and minerals (Frost and McCammon, 2008).

**Acknowledgements:**



Always consult and cite the final, published document. See http:/www.minsocam.org or GeoscienceWorld

M.M. Reagan, A.E. Gleason, and W.L. Mao are supported by the NSF Geophysics Program (EAR-1446969). We thank Paul Chow (APS), Alastair MacDowell (ALS), and Jinyuan Yan (ALS) for their assistance with the synchrotron experiments, and Jinfu Shu (Geophysical Lab) for help with sample loading. Portions of this work were performed at beamline 12.2.2 of ALS, LBNL. ALS is supported by the Director, Office of Science, Office of Basic Energy Sciences (BES), of the U.S. Department of Energy (DOE) under Contract No. DE-AC02-05CH11231. Portions of this work were also performed at HPCAT (Sector 16), APS, ANL. HPCAT operations are supported by DOE-NNSA under Award No. DE-NA0001974 and DOE-BES under Award No. DE-FG02-99ER45775, with partial instrumentation funding by NSF. APS is a DOE-BES User Facility operated for the DOE Office of Science by ANL under Contract No. DE-AC02-06CH11357.

**References:**

Bolotina, N., Molchanov, V., Dyuzheva, T., Lityagina, L., and Bendeliani, N., (2008). Single- crystal structures of high-pressure phases FeOOH, FeOOD, and GaOOH. Crystallography Reports. 53 (6), 960–965.

Benoit, M., Marx, D., and Parrinello, M. (1998). Tunnelling and zero-point motion in high-pressure ice. Nature, 392(6673), 258–261.

Birch, F. (1978). Finite Strain Isotherm and Velocities for Single-Crystal and Polycrystalline NaCl at High Pressures and 300°K. Journal of Geophysical Research, 83(B3), 1257–1268.

Friedrich, A., Haussül, E., Boehler, R., Morgenroth, W., Juarez-Arellano, E. a., and Winkler, B. (2007). Single-crystal structure refinement of diaspore at 50 GPa. American Mineralogist, 92(10), 1640–1644.

Frost, D. J., and McCammon, C. a. (2008). The Redox State of Earth's Mantle. Annual Review of Earth and Planetary Sciences, 36(1), 389–420.

Gerth, J. (1990). Unit-cell Dimensions of Pure and Trace Metal-associated Goethites. Geochimica et Cosmochimica Acta, 54(2), 363–371.



Always consult and cite the final, published document. See http:/www.minsocam.org or GeoscienceWorld

Gilli, G. and Gilli, P. (2009) The Nature of the Hydrogen Bond, Oxford University Press, New York. □

Gleason, A. E., Jeanloz, R., and Kunz, M. (2008). Pressure-temperature stability studies of FeOOH using X-ray diffraction. American Mineralogist, 93(11-12), 1882–1885.

Gleason, A. E., Quiroga, C. E., Suzuki, A., Pentcheva, R., and Mao, W. L. (2013). Symmetrization driven spin transition in ε-FeOOH at high pressure. Earth and Planetary Science Letters, 379, 49–55.

Hammersley, A. P. (1998). Fit2D: V99.129 Reference Manual Version 3.1. Internal Report ESRF – 98 – HA01.

Heinz, D., and Jeanloz, R. (1984). The equation of state of the gold calibration standard. Journal of Applied Physics, 55(June 1983), 885–893.

Holzapfel, W. B. (1972). Symmetry of the hydrogen bonds in Ice VII. Journel of Chemical Physics, 56(2), 712–715.

Kosmulski, M., Maczka, E., Jartych, E., and Rosenholm, J. B. (2003). Synthesis and characterization of goethite and goethite-hematite composite: Experimental study and literature survey. Advances in Colloid and Interface Science, 103(1), 57–76.

Lin, J.F, Speziale, S., Mao, Z., and Marquardt, H. (2013). Effects of the Electronic Spin Transitions of Iron in Lower Mantle Minerals□: Implications for Deep Mantle Geophysics and Geochemistry. Reviews of Geophysics, 51(2), 244–275.

Lin, J.F., and Tsuchiya, T. (2008). Spin transition of iron in the Earth's lower mantle. Physics of the Earth and Planetary Interiors, 170(3-4), 248–259.

Lin, J.F., Vankó, G., Jacobsen, S. D., Iota, V., Struzhkin, V. V., Prakapenka, V. B., Kuznetsov, A., and Yoo, C.-S. (2007). Spin transition zone in Earth's lower mantle. Science, 317(5845), 1740–3.

Lutterotti, L., Matthies, S., Wenk, H.-R., Schultz, A. S., and Richardson, J. W. (1997). Combined texture and structure analysis of deformed limestone from time-of-flight neutron diffraction spectra, Journel of Appied Physics, 81, 594–600.

Mao, H. K., Xu, J., and Bell, P. M. (1978). High Pressure Physics: Sustained Static Generation of 1.36 to 1.72 Megabars. Science. 200(4346).

Mattila, A., Pylkkänen, T., Rueff, J-P., Huotari, S., Vankó, G., Hanfland, M., Lehtinen, M., and Hämäläinen, K. (2007). Pressure induced magnetic transition in siderite FeCO3 studied by x-ray emission spectroscopy. Journal of Physics, 19(38), 386206.



Always consult and cite the final, published document. See http:/www.minsocam.org or GeoscienceWorld

Momma, K., and Izumi, F., (2008). VESTA: a three-dimensional visualization system for electronic and structural analysis. Journel of Appied Crystallography, 41, 653–658.386206.

Otte, K., Pentcheva, R., Schmahl, W. W., and Rustad, J. R. (2009). Pressure-induced structural and electronic transitions in FeOOH from first principles. Physical Review B, 80(20), 205116.

Sano, A., Ohtani, E., Kubo, T., and Funakoshi, K. I. (2004). In situ X-ray observation of decomposition of hydrous aluminum silicate AlSiO3OH and aluminum oxide hydroxide d-AlOOH at high pressure and temperature. Journal of Physics and Chemistry of Solids, 65, 1547–1554.

Skoog, D.A., West, D.M., and Holler, F.J., (1996). Fundamentals of Analytical Chemistry, 7th Edition, Thomson Learning, Inc, USA.

Speziale, S., Milner, a, Lee, V. E., Clark, S. M., Pasternak, M. P., and Jeanloz, R. (2005). Iron spin transition in Earth's mantle. Proceedings of the National Academy of Sciences of the United States of America, 102(50), 17918–22.

Stackhouse, S., Brodholt, J. P., and Price, G. D. (2007). Electronic spin transitions in iron-bearing $MgSiO_3$ perovskite. Earth and Planetary Science Letters, 253(1-2), 282–290.

Suzuki, A. (2010). High-pressure X-ray diffraction study of epsilon-FeOOH. Physics and Chemistry of Minerals, 37(3), 153–157.

Schwertmann, U., and R.M. Cornell, R.M., (2000). The Iron Oxides in the Laboratory, 2nd edition, Wiley-VCH, Weinheim.

Voigt, R. and Will, G. (1981). The system Fe2O3-H2O under high pressures. Neues Jahrbuch fur Mineralogie, 2, 89–96.

Wang, X., Chen, X., Gao, L., Zheng, H., Ji, M., Tang, C., Shen, T., and Zhang, Z., (2004). Synthesis of b -FeOOH and a -Fe2O3 nanorods and electrochemical properties of b -FeOOH, Journel of Material Chemistry, 905–907.

Williams, Q., and Hemley, R. (2001). Hydrogen in the deep Earth. Annual Review of Earth and Planetary Sciences, 29. 365–418.

Xu, W., Greenberg, E., Rozenberg, G. K., Pasternak, M. P., Bykova, E., Boffa-Ballaran, T., Dubrovinsky, L., Prakapenka, V., Hanfland, M., Vekliova, O. Simak, S., and Abrikosov, I. A. (2013). Pressure-Induced Hydrogen Bond Symmetrization in Iron Oxyhydroxide. Physical Review Letters, 111(17), 175501.



Always consult and cite the final, published document. See http:/www.minsocam.org or GeoscienceWorld

342 **Tables:**

343 **Table 1**. A comparison of unit cell volume, bulk modulus, and the spin transition
344 pressure for the FeOOH polymorphs. The pressure-volume data for all the phases were fit
345 to a 2nd order Birch-Murnaghan equation of state.

346

| Phase | $V_0$/ f.u. (Å$^3$) | $K_0$ (GPa) | Spin Transition Pressure (GPa) |
|---|---|---|---|
| $\alpha$* | 34.6 (3) | 120 (3) | 49 |
| $\beta$ | 42.1 (3) | 283.6 (11) | N/A |
| $\gamma$ | 36.9 (2) | 103.5 (10) | 36 |
| $\varepsilon$** | 33.2 (5) | 158 (5) | 49 |

347

348 * Xu et al., 2013

349 **Gleason et al., 2008

350

351

352

353

354

355

356

357

358

359

360



Always consult and cite the final, published document. See http:/www.minsocam.org or GeoscienceWorld

361 **Table 2**. A comparison of the experiments performed in this study.

362

| Phase | Technique (Beamline) | Specifications | | | Highest Pressure (GPa) |
|---|---|---|---|---|---|
| | | Gasket | Pressure Medium | X-ray wavelength / energy | |
| $\alpha$ | XES (16-IDD, APS) | Be | None | 11.3keV | 85 |
| $\beta$ | XES (16-IDD, APS) | Be | None | 11.3keV | 65 |
| $\beta$ | XRD (16-BM-D, APS; 12.2.2 ALS) | Stainless Steel | Silicone Oil | 0.4133 Å 0.4246 Å | 29 |
| $\gamma$ | XES (16-IDD, APS) | Be | None | 11.3keV | 64 |
| $\gamma$ | XRD (12.2.2, ALS) | W | Silicone Oil | 0.4246 Å | 34 |

363

364

365 **Figures:**



Always consult and cite the final, published document. See http:/www.minsocam.org or GeoscienceWorld

This is a preprint, the final version is subject to change, of the American Mineralogist (MSA)
Cite as Authors (Year) Title. American Mineralogist, in press.
(DOI will not work until issue is live.) DOI: http://dx.doi.org/10.2138/am-2016-5449

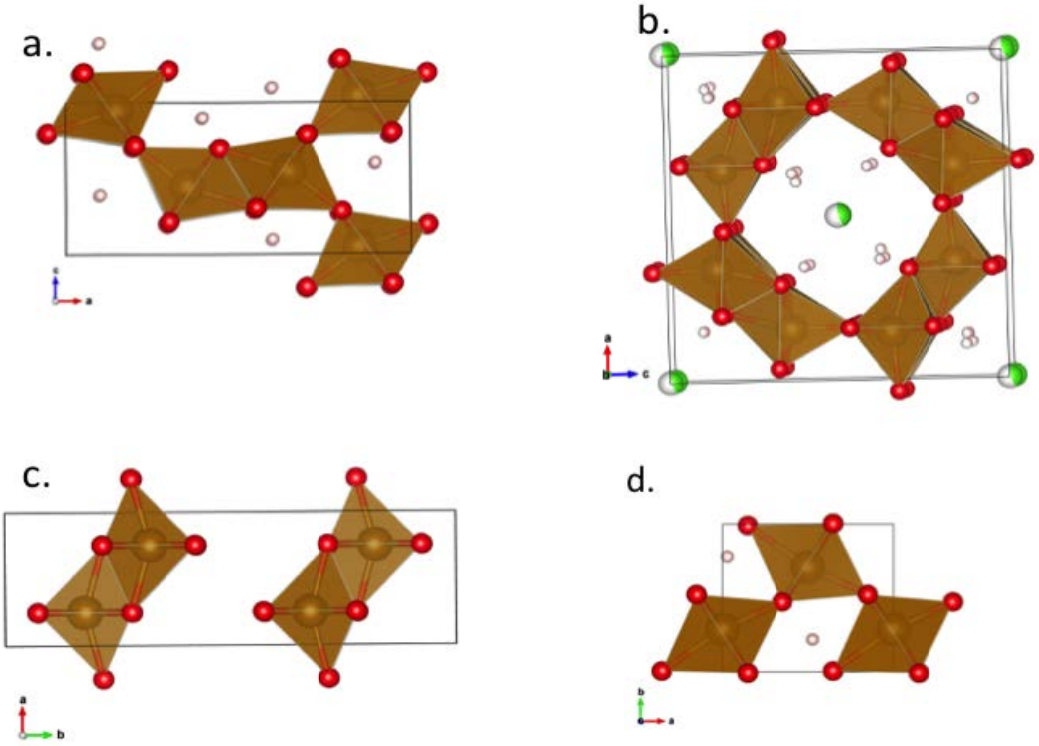


372
373 **Figure 1.** The ambient pressure crystal structures of the FeOOH polymorphs showing
374 iron (gold), oxygen (red), hydrogen (light pink), chlorine (green), and $FeO_3(OH)_3$
375 octahedra (tan). (a) $\alpha$-FeOOH (goethite), (b) $\beta$-FeOOH (akaganeite), (c) $\gamma$- FeOOH
376 (lepidocrocite) and (d) $\varepsilon$–FeOOH. These structures were generated using VESTA
377 (Momma et al., 2008).
373



Always consult and cite the final, published document. See http:/www.minsocam.org or GeoscienceWorld

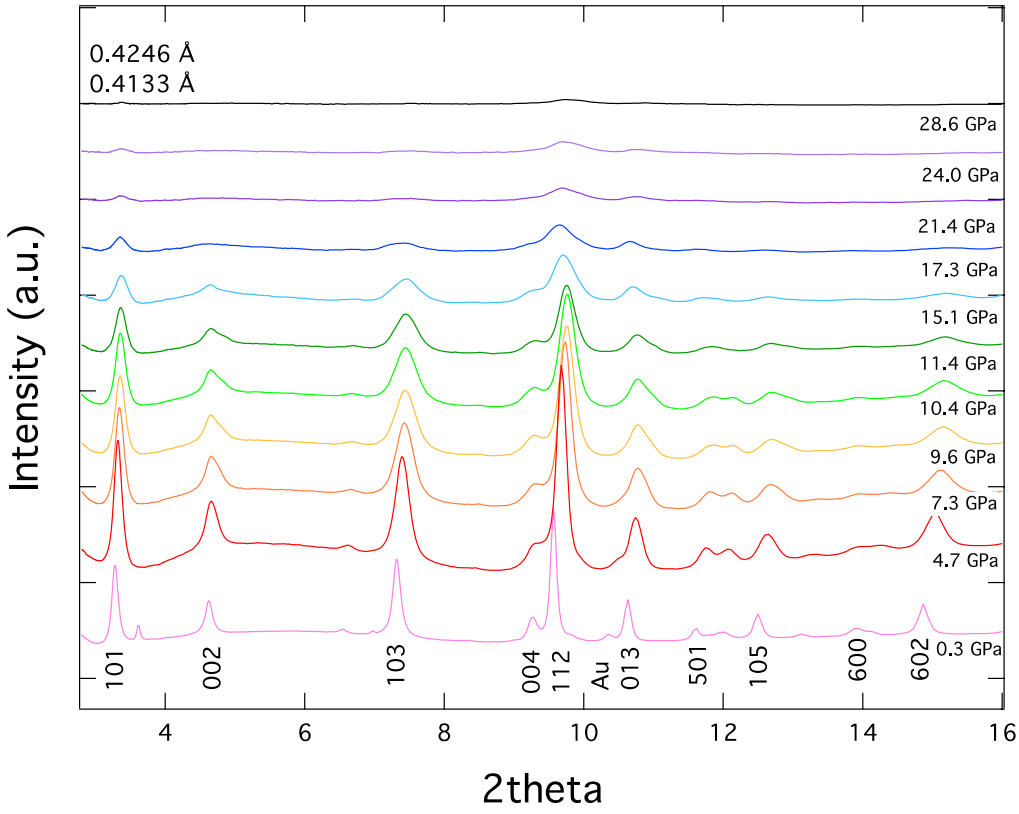


373

374

375

376 **Figure 2.** XRD spectra for $\beta$-FeOOH for selected pressures. The sample becomes
377 amorphous above ~17 GPa. $\lambda$= 0.4133 Å 0.3 GPa- 15.1 GPa and 0.4246 Å above 17.3
378 GPa.



Always consult and cite the final, published document. See http:/www.minsocam.org or GeoscienceWorld

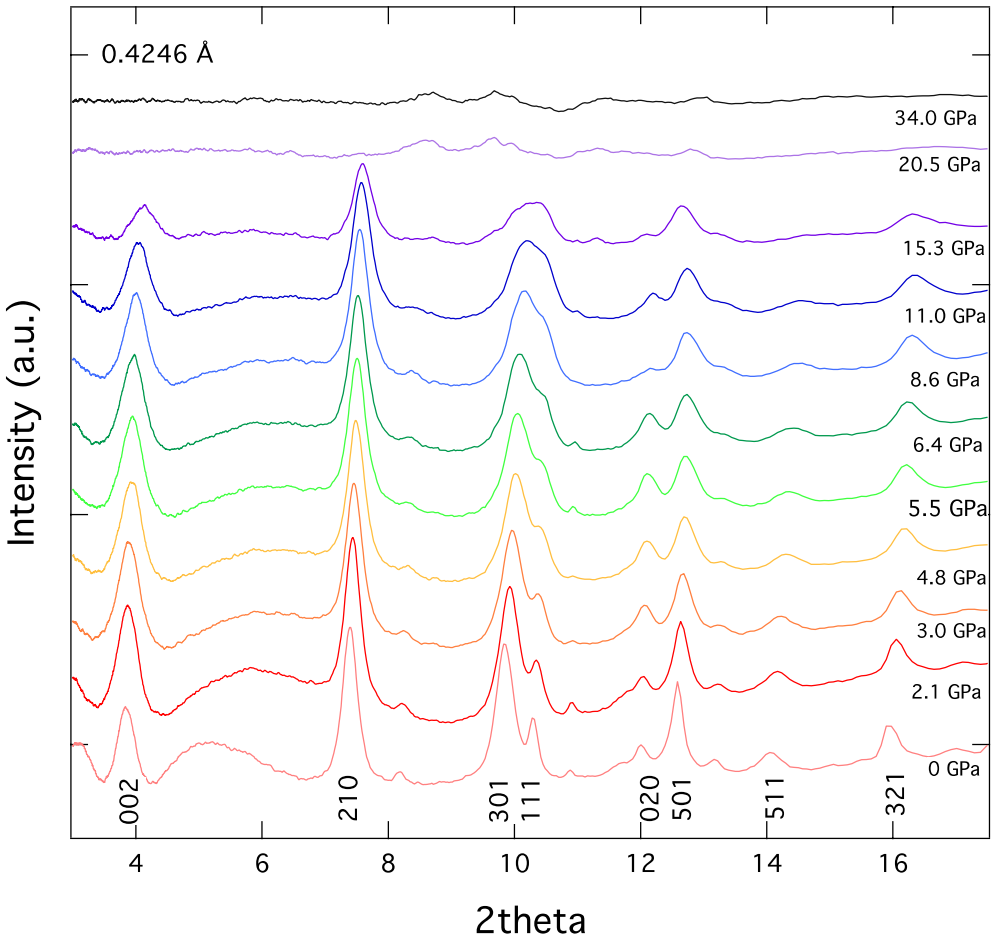


379

380 **Figure 3.** XRD spectra for $\gamma$-FeOOH for select pressures. It becomes amorphous above
381 ~20 GPa. $\lambda$= 0.4246 Å.



Always consult and cite the final, published document. See http:/www.minsocam.org or GeoscienceWorld

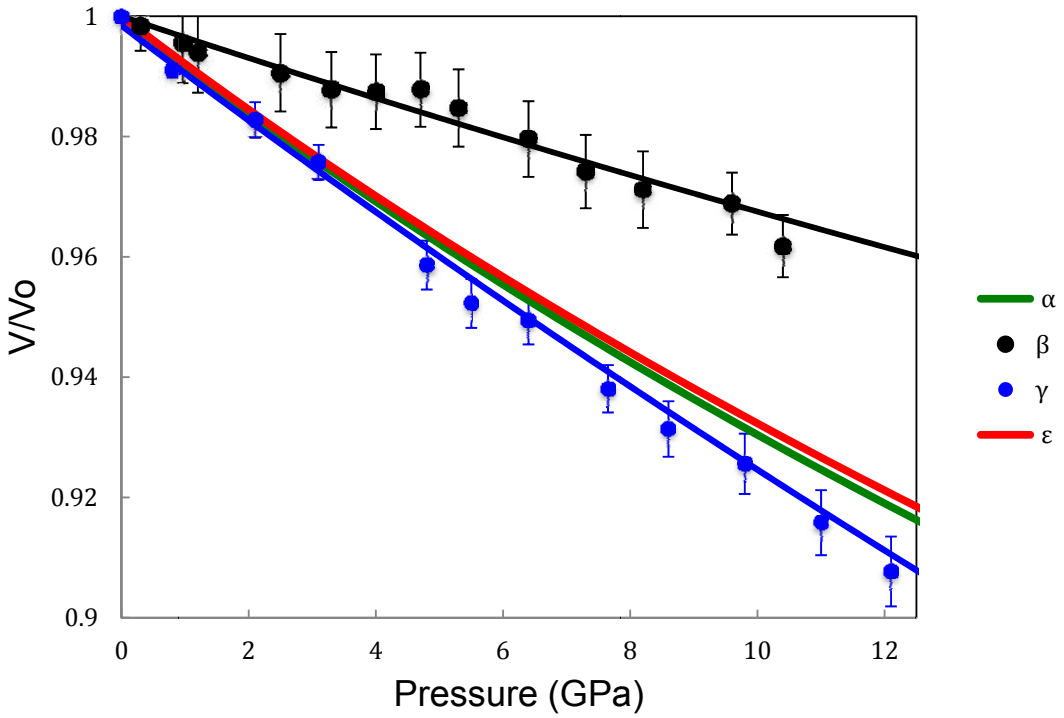


383

388 **Figure 4.** EOS for the FeOOH polymorphs. $\alpha$ and $\varepsilon$ are plotted for comparison from
389 previous published results (Xu et al., 2013; Gleason et al., 2008). Note the lower
390 compressibility for $\beta$-FeOOH reflecting its higher $K$ values. Both the $\beta$ and $\gamma$ phases
391 become amorphous and their XRD spectra cannot be fit to a crystalline structure at higher
392 pressures.



Always consult and cite the final, published document. See http:/www.minsocam.org or GeoscienceWorld

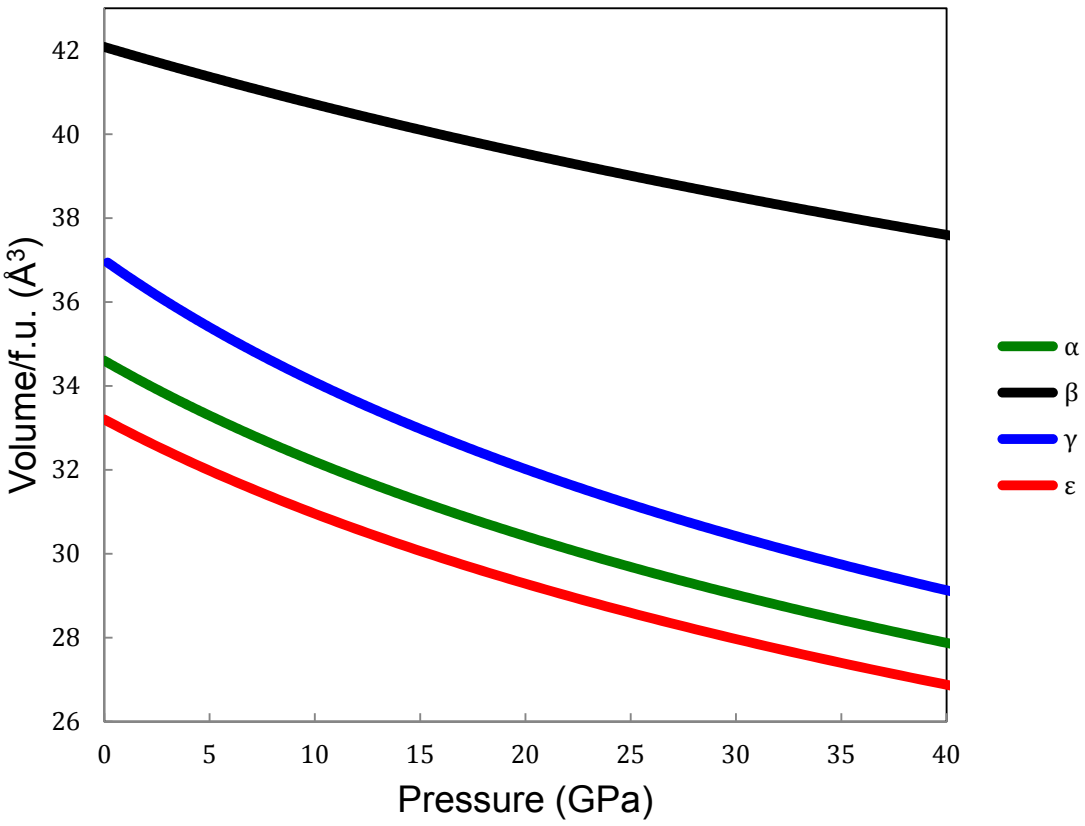


388

389 **Figure 5.** Volume per formula unit (f.u.) as a function of pressure. *β*–FeOOH has a
390 significantly larger volume compared to the other three polymorphs.



Always consult and cite the final, published document. See http:/www.minsocam.org or GeoscienceWorld

This is a preprint, the final version is subject to change, of the American Mineralogist (MSA)
Cite as Authors (Year) Title. American Mineralogist, in press.
(DOI will not work until issue is live.) DOI: http://dx.doi.org/10.2138/am-2016-5449

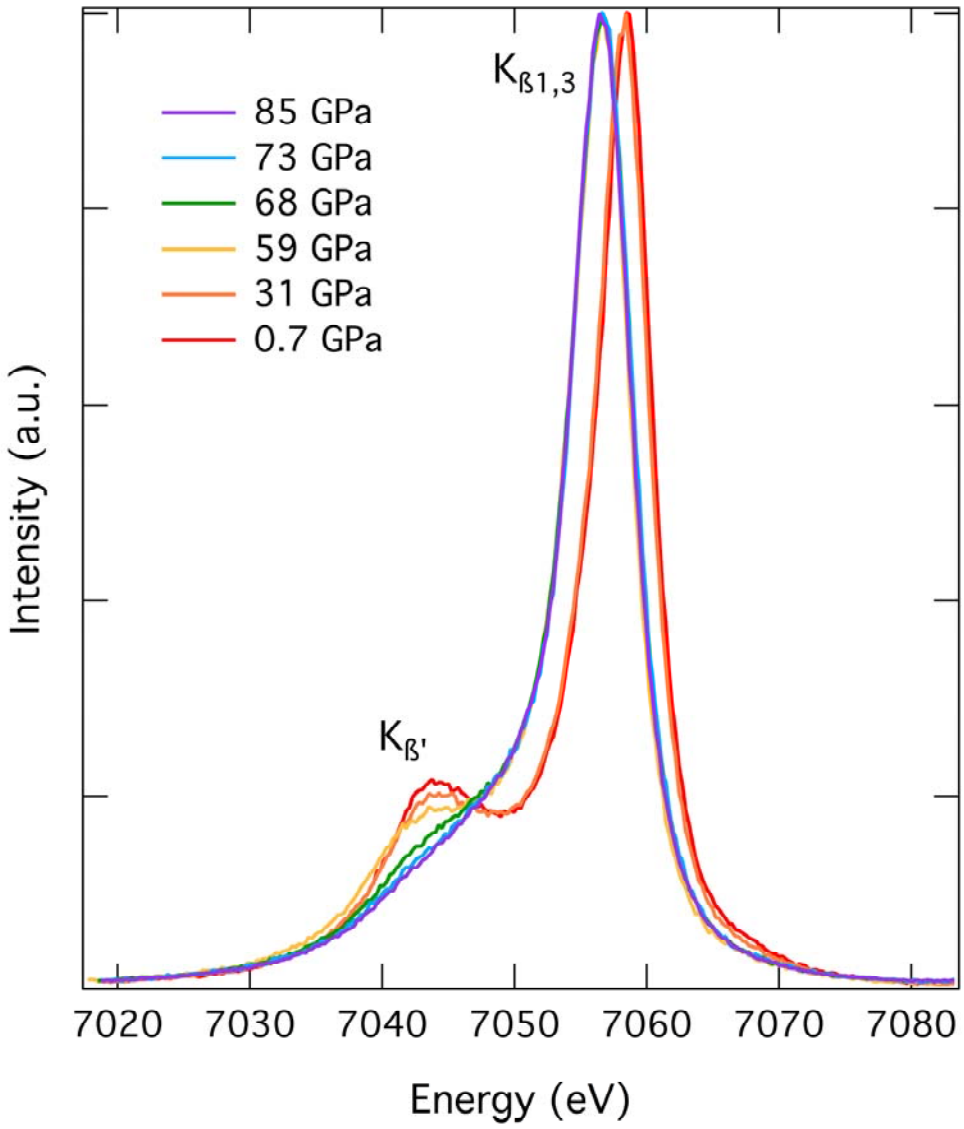


**Figure 6**. $K_\beta$ emission spectra as a function of pressure for $\alpha$-FeOOH.



Always consult and cite the final, published document. See http:/www.minsocam.org or GeoscienceWorld

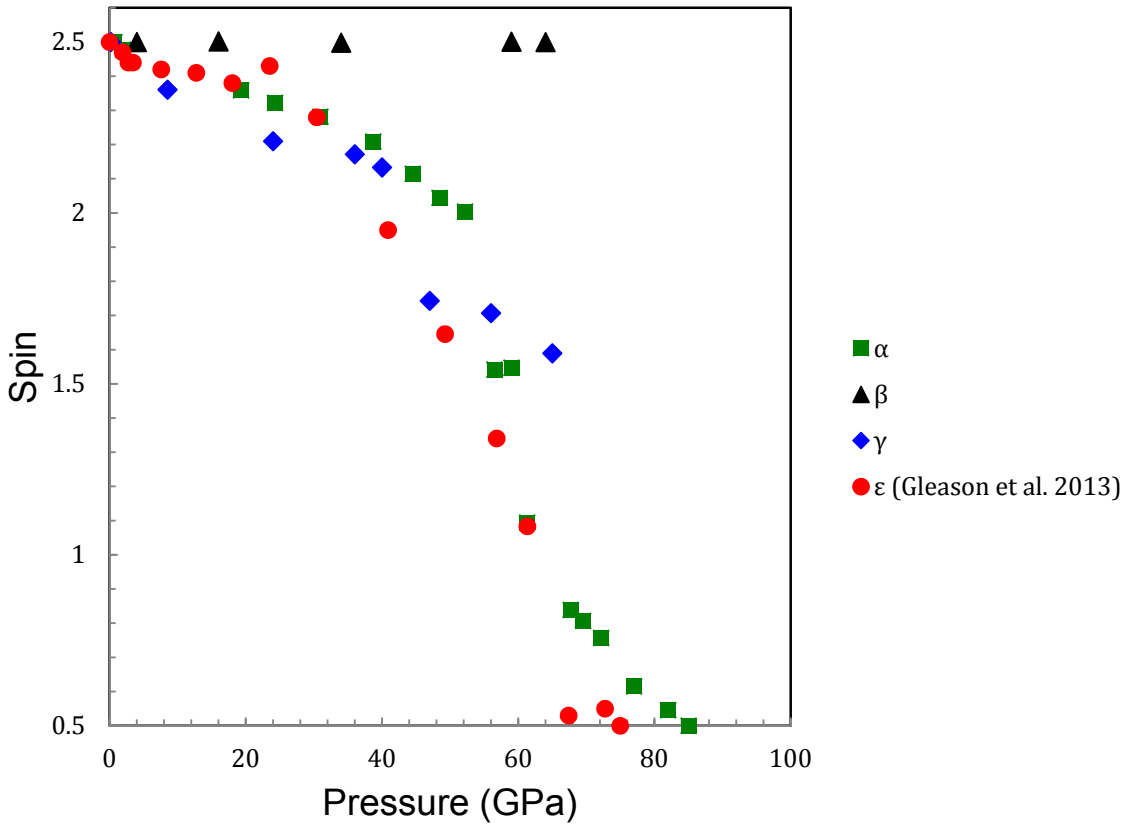


397

398 **Figure 7**. Average spin number as a function of pressure for *α*-FeOOH (green squares),
399 *β*-FeOOH (black triangles), *γ*-FeOOH (blue diamonds) using the IAD method (Mattila et
400 al., 2007). The low spin state for *α*-FeOOH was used to calculate the IAD values for *β*-
401 FeOOH and *γ*-FeOOH. ε-FeOOH XES data from Gleason et al. (2013) was added (red
402 circles). The spin transition for *α*-FeOOH begins at ~50 GPa.



Always consult and cite the final, published document. See http:/www.minsocam.org or GeoscienceWorld

This is a preprint, the final version is subject to change, of the American Mineralogist (MSA)
Cite as Authors (Year) Title. American Mineralogist, in press.
(DOI will not work until issue is live.) DOI: http://dx.doi.org/10.2138/am-2016-5449

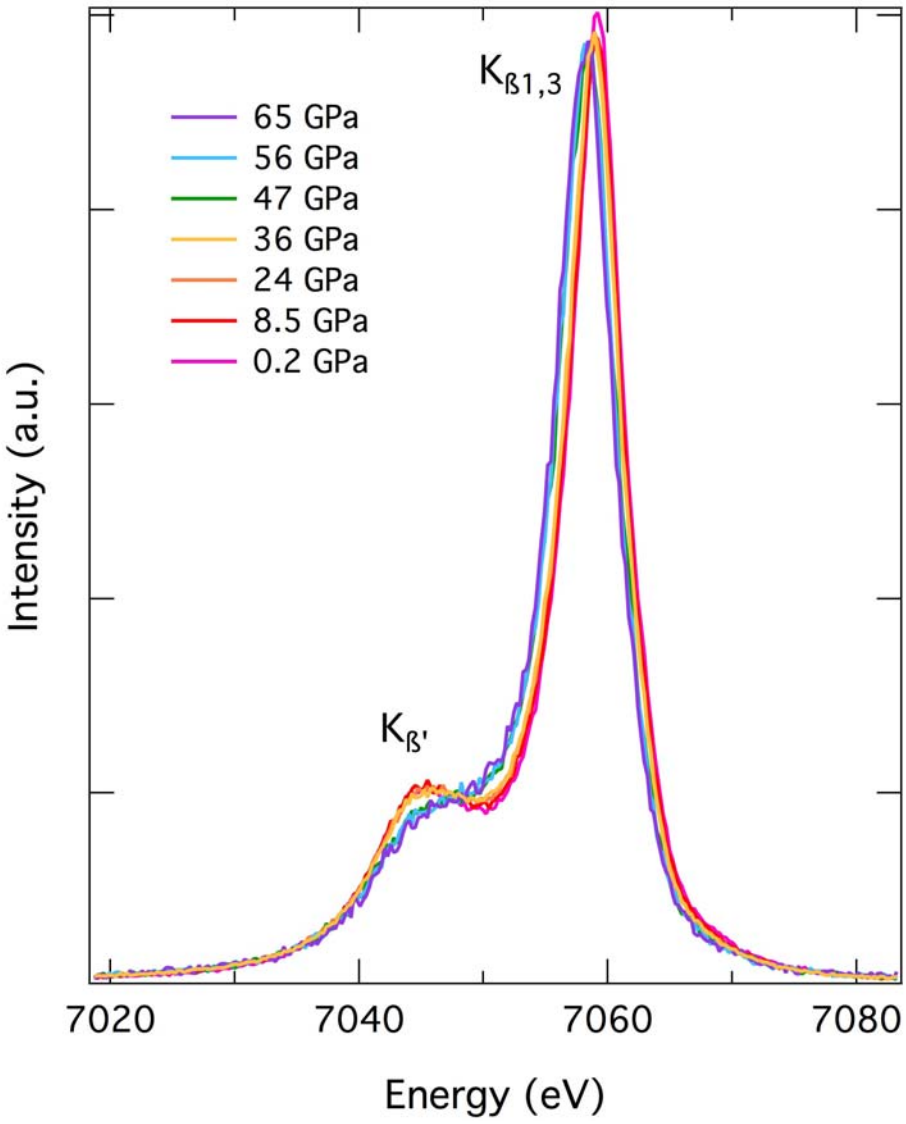


403

404 **Figure 8**. $K_\beta$ emission spectra as a function of pressure for $\gamma$-FeOOH.

405



Always consult and cite the final, published document. See http:/www.minsocam.org or GeoscienceWorld

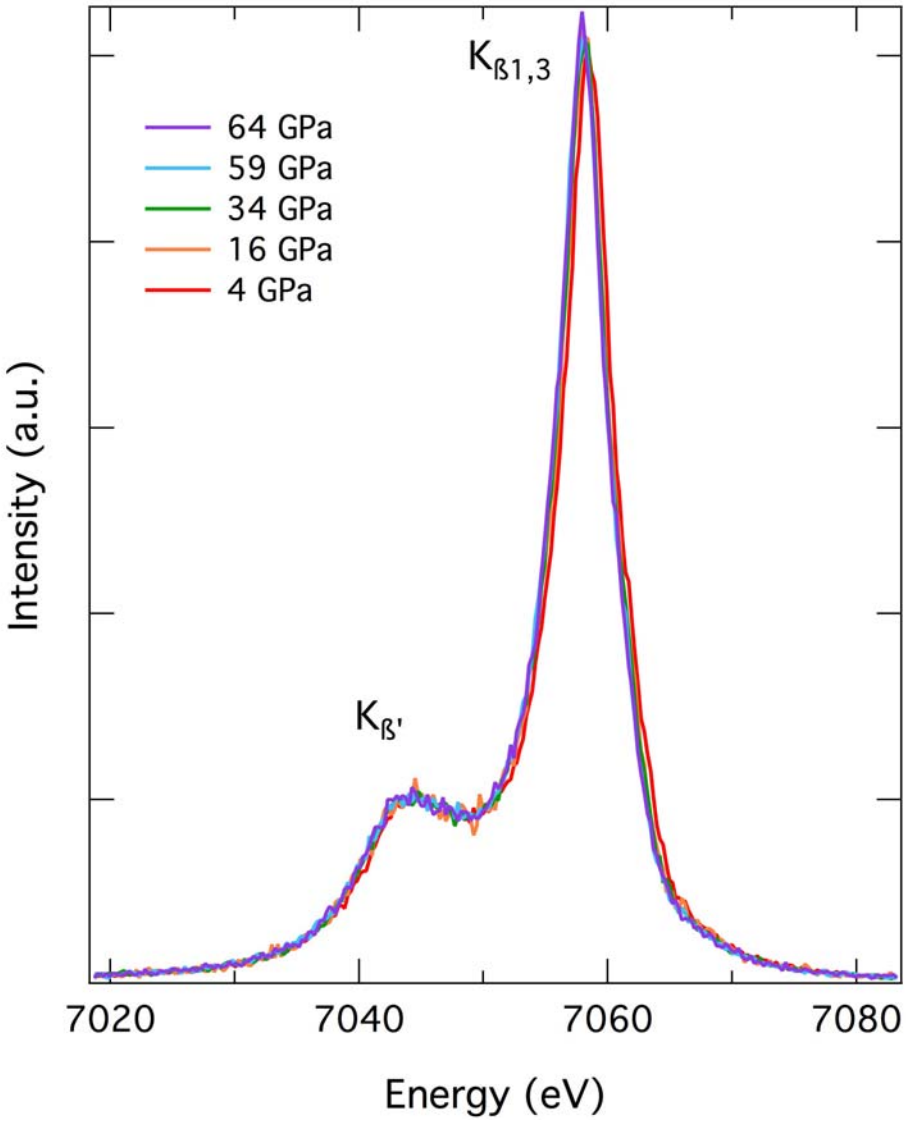


406

407

408 **Figure 9.** $K_\beta$ emission spectra as a function of pressure for $\beta$-FeOOH.



Always consult and cite the final, published document. See http:/www.minsocam.org or GeoscienceWorld